# A Non-Modal Structural-Damage-Location Method and its Application

M. Oeljeklaus
Curt-Risch Institute, University of Hannover,
Appelstr. 9A, 30167 Hanover, Germany

B. Powalka
Institute of Manufacturing Engineering, Technical University of Szczecin,
Piastow 19, 70310 Szczecin, Poland

April 4, 2003

**ABSTRACT**

This paper[1] is on model based structural damage location, i.e. on damage location based on measurements taken from a structure as well as on a mathematical model of the structure for the purpose of diagnosis, simulation and identification. Since this model has to be reliable the model parameters have to be identified and updated. This adjustment of the parameters by means of measured data, i.e. model correction within system identification, is in general an ill-posed inverse problem which often has to be solved with incomplete output measurements with respect to the nodes of the underlying finite element model ([1], [2],[3], [4], [5], [6], [7]). The problem of incompleteness can be handled by projection methods introduced first in [3] and thus avoiding a model reduction. This method, the Projective Input Residual Method (PIRM), is an identification method based on input and incomplete output measurements in the frequency domain. Using the projection methods of the PIRM in [8] a damage indicator was defined and applied. This indicator was shown to be sensitive to system modifications, e.g. decreased stiffness due to a damage, using only a small fraction of the total number of possible measuring points. Further application and analysis of this indicator including regularization methods was done in [9].

Since the computation amount to calculate the necessary projections for the hole mathematical model is growing rapidly with the number of degrees of freedom in this contribution a generalisation of this indicator is introduced which is appropriate for subsystem monitoring and subsystem damage location. Especially the evaluation of the indicator values for the parameters under investigation becomes more efficient in the framework of monitoring.

The method and its underlying theory is presented and illustrated by a laboratory example, a gantry robot. The structure was objected to real damage and the underlying input-output measurements where taken for both states of the structures, the healthy and the damaged. The results presented underline the sensitivity of the presented generalized indicator to system modifications and damage location.

[1]This work is part of the collaborative research center 477 in Braunschweig, Germany, and as such supported by the DFG, the Deutsche Forschungsgesellschaft.

# 1 NOMENCLATURE

The following nomenclature lists symbols and their meaning that are used in this paper:

| | |
|---|---|
| $R(W)$ | image space of the linear map $W$ generated by the columns of $W$ |
| $\bar{R}(W)$ | orthogonal complement of $R(W)$ |
| $N(W)$ | kernel or null space of the linear map $W$ |
| $\bar{N}(W)$ | orthogonal complement of $N(W)$ |
| $n_p$ | number of parameters to be identified |
| $\nu$ | indices for a parameter component |
| $m$ | number of measured output components |
| $a$ | variable parameter vector |
| $a^0$ | sought parameter of the true model |
| $\mathbb{1}$ | $= (1, \ldots, 1)^T$ start parameter vector by definition |
| $e_\nu$ | $\in \mathbb{R}^{n_p}:$ $\nu$th parameter unity vector |
| $B^\dagger$ | Moore-Penrose or generalized inverse of a matrix $B$ |
| $B^H$ | $= B^{*T}$conjugate transpose of a matrix $B$ |
| $C$ | $\in \{0,1\}^{m\times n}$ measurement matrix, selects measured rows, i.e. left-multiplication with $C$ eliminates rows that correspond to non measured components |
| $\bar{C}$ | $\in \{0,1\}^{(n-m)\times n}$ complementary measurement matrix, selects non-measured rows: $C\bar{C}^T = 0_{m\times(n-m)}$ |
| $I_k$ | $k \times k$ identity matrix |
| $S_\omega(a)$ | dynamic stiffness matrix for frequency $\omega$ |
| $F_\omega(a)$ | $= (S_\omega(a))^{-1}$ frequency response matrix |

# 2 INTRODUCTION

The parameters of our underlying mathematical model are the physical parameters of an elastomechanical system, i.e. the mass, damping and stiffness matrices and its components. Since the calculation of all the elements of these parameter matrices is computationally too expensive we apply the well-known parameter topology as defined in [2] which uses a low-dimensional ($n_p \ll n^2/2$) subbase of the space of the system matrices, presuming that the sought true model may be well approximated in the corresponding model subspace: The mass, damping and stiffness matrices of the start model are assembled from sparsely occupied, symmetric matrices of full system dimension, i.e. $n \times n$:

$$M = \sum_{\sigma\in\mathcal{M}} A_\sigma, \quad B = \sum_{\rho\in\mathcal{B}} A_\rho, \quad K = \sum_{\iota\in\mathcal{K}} A_\iota. \tag{1}$$

We have $\mathcal{M} \cup \mathcal{B} \cup \mathcal{K} = \{1, \ldots, n_p\}$, where the elements of the sets $\mathcal{M}$, $\mathcal{B}$ and $\mathcal{K}$ are the parameter indices of the mass, damping and stiffness summand matrices.

The mathematical model consists of all linear combinations of these base matrices, i.e. given a parameter vector $a = (a_1, \ldots, a_{n_p})$ we have for the model:

$$M(a) := \sum_{\sigma\in\mathcal{M}} a_\sigma A_\sigma, \quad B(a) := \sum_{\rho\in\mathcal{B}} a_\rho A_\rho, \quad K(a) := \sum_{\iota\in\mathcal{K}} a_\iota A_\iota \tag{2}$$

Thus the dynamic stiffness matrices of the model is:

$$S_\omega(a) = -\omega^2 M(a) + j\omega B(a) + K(a) = \sum_{\nu=1}^{n_p} a_\nu S_\omega(e_\nu) \tag{3}$$

Remark: For given $\omega > 0$ the set of dynamic stiffness matrices

$$\mathcal{S}_{\mathbf{R}}^{\omega} := \left\{ S_\omega(a) \in \mathbb{C}^{n\times n} : a \in \mathbb{R}^{n_p} \right\} \tag{4}$$

is a real vector space of dimension $n_p$ generated by the base of elementary dynamic stiffness matrices $S_\omega(e_1), \ldots, S_\omega(e_{n_p})$.

For further investigations we assume the following general experimental design in the frequency domain:

**A:** $N \geq 1$ excitation frequencies $\omega_1, \ldots, \omega_N$, and $2N$ matrices $P_1^\mu, U_1^\mu, \ldots P_N^\mu, U_N^\mu$, each having $n$ rows and a varying number of linearly independent columns $m_1, \ldots, m_N$: the $m_r$ columns of $P_r^\mu$ and $U_r^\mu, r = 1, \ldots, N$, are (respectively) the excitation and associated (complete) response vectors for the frequencies $\omega_r, r = 1, \ldots, N$ which are created by the corresponding frequency response matrices: $U_1^\mu = F_{\omega_1}(a^0)P_1^\mu, \ldots, U_N^\mu = F_{\omega_N}(a^0)P_N^\mu$. (The upper index $^\mu$ in $U^\mu$ or $P^\mu$ is an abbreviation of the known measurements, i.e. all objects having this superscript are constant objects coming from the experimental design. In contrast, an upper index $^\gamma$ as in $P^\gamma$ is used in cases of objects that are calculated as a function of $a$, $P^\gamma = P^\gamma(a)$.

**B:** The measured output vectors with respect to the measurement matrix $C$ are the columns of the matrices $CU_r^\mu = CF_{\omega_r}(a^0)P_r^\mu, \quad r = 1, \ldots, N$, with $a^0$ as the true model parameter.

**C:** For an arbitrary parameter $a$, $CU_r^\gamma(a) := CF_{\omega_r}(a)P_r^\mu, \quad r = 1, \ldots, N$, are the corresponding calculated output vectors, and are also incomplete.

In the following we assume for an arbitrary but fixed $1 \leq r \leq N$: $\omega := \omega_r$, $P^\mu := P_r^\mu$ and $CU^\mu := CU_r^\mu$. Furthermore, we assume $m \ll n$ for the row dimension of the measurement matrix $C$.

# 3 SUBSYSTEM ADAPTATION OF THE PROJECTIVE INPUT RESIDUAL METHOD

After a short introduction to the Projective Input Residual Method (PIRM) we will present its adaptation for subsystem damage identification.

Due to the linear independence of the elementary dynamic stiffness matrices $\{S_\omega(e_\nu), \nu = 1, \ldots, n_p\}$ the map $a \longmapsto S_\omega(a)$ between the real vector space of $n_p$-vectors and the space of parametrized dynamic stiffness matrices $\mathcal{S}_{\mathbf{R}}^{\omega}$ is an isomorphism. In consequence $a^0$ and $S_\omega(a^0)$ are the same objects w.r.t. this isomorphism, i.e. $a^0 \equiv S_\omega(a^0)$. Remark: Two vector spaces E, F are said to be isomorphic if there exists an isomorphism of E onto F. In that case, any theorem proved for E, involving vectors and subspaces of E, immediately gives a corresponding theorem for F, involving the images of the vectors and subspaces in question (see [10]). This is an important fact, since it implies that hunting for $a^0$ (and this is what we do) means hunting for $S_\omega(a^0)$ as it is done by the classical input residual method which may be applied as the minimization of the $L_2$-norm of the input residuals $P^\mu - S_\omega(a)U^\mu$ if all output components were measured, i.e. $C = I_n$ and $m = n$. The minimization must be performed by solving the associated normal equations, i.e. the associated overdetermined system of linear equations for $a$. If $C \neq I_n$, i.e. not all components have been measured, given an arbitrary parameter $a$ we can write

$$S_\omega(a)U^\mu = \underbrace{[S_\omega(a)C^T][CU^\mu]}_{T_M} + \underbrace{[S_\omega(a)\bar{C}^T][\bar{C}U^\mu]}_{T_U}, \tag{5}$$

where $T_M$ can be evaluated since $CU^\mu$ was measured and $T_U$ can not be evaluated. But what we know is that $T_U$ is an element of $X(\omega, a) := R(S_\omega(a)\bar{C}^T)$, the $n-m$-dimensional image space of the linear operator $S_\omega(a)\bar{C}^T$.

Thus, as a generalization of the classical input residual method, we eliminate the uncertainty in (5) by using the quotient vector space $D(\omega, a) := \mathbb{C}^n / X(\omega, a)$ in which the cosets of all elements of $X(\omega, a)$ including $T_U$ vanish and thus the evaluation of $S_\omega(a)U^\mu$ in terms of cosets of $D(\omega, a)$ is unique. As can be shown, the classical input residual method applied in the family of factor spaces $\{D(\omega, a)\}_{a \in \mathbf{R}^{n_p}}$ is to find $a$ that minimizes the distance between $P^\mu$, the experimental input, and the $m$-dimensional orthogonal complement of the space $X(\omega, a)$. We get the following PIRM definition equations with, in contrast to the classical input residual method, nonlinear residuals $v(a)$:

$$\text{Find } \hat{a} = \operatorname{argmin}_a \|v(a)\|^2 \text{ with} \tag{6}$$

$$v(a) = P(a) \underbrace{\left(P^\mu - S_\omega(a) C^T C U^\mu\right)}_{=:\Phi(\omega,a)}. \tag{7}$$

The operator $P(a)$ is the projector to the orthogonal complement of $X(\omega, a) = N(CF_\omega(a))$ and therefore the map $a \mapsto P(a)$ is nonlinear. Due to assumption **B** on page 3, $\Phi(\omega, a^0)$ is an element of $N(CF_\omega(a^0))$ and thus vanishes in $D(\omega, a^0)$. In consequence we have $v(a^0) = 0$ and the method is shown to be asymptotically unbiased.

The following adaptation to subsystems of the PIRM-residuals $v(a)$ as defined in (7) will be used in the next section to define a damage indicator that can be used to indicate and locate damages during online monitoring.

For this purpose let $Q \in \{0,1\}^{l \times n}$, similar to the measurement matrix $C$, be a matrix whose left multiplication with $S_\omega(a)$ or $F_\omega(a)$ selects certain rows of this matrices: Let Q select the rows of a certain $l$-dimensional subsystem and assume that the measured components are contained in this subsystem implying $l > m$. Furthermore we assume the measurement matrix $C$ to select the measured components/rows within this subsystem und not within the whole system, i.e. $C \in \{0,1\}^{m \times l}$ instead of $C \in \{0,1\}^{m \times n}$. Also the experimental input and output measurements are assumed to be of subsystem dimension, i.e. the corresponding vectors $P^\mu$ and $U^\mu$ are of length $l$. Then we can write for the part of the dynamic stiffness matrix that corresponds to the subsystem

$$S_Q(\omega, a) := Q S_\omega(a) Q^T, \tag{8}$$

If Q selects a slightly coupled subsystem we can further assume to have approximately

$$S_Q(\omega, a)^{-1} = \left(Q S_\omega(a) Q^T\right)^{-1} \tag{9}$$

$$= Q S_\omega(a)^{-1} Q^T - \overbrace{[Q F_\omega(a) \bar{Q}^T][\bar{Q} F_\omega(a) \bar{Q}^T]^{-1}[\bar{Q} F_\omega(a) Q^T]}^{\approx 0, \text{ if subsystem is slightly coupled}} \tag{10}$$

$$\approx Q \left(S_\omega(a)\right)^{-1} Q^T = \underbrace{Q F_\omega(a) Q^T}_{F_Q(\omega,a)} \tag{11}$$

A proof for equation (10) can be found in [11]. In adaptation of equation (5) we get the following calculated input for our subsystem

$$Q S_\omega(a) Q^T U^\mu = \underbrace{[Q S_\omega(a) Q^T C^T][C U^\mu]}_{T_M^Q} + \underbrace{[Q S_\omega(a) Q^T \bar{C}^T][\bar{C} U^\mu]}_{T_U^Q}, \tag{12}$$

Thus the adaptation $v_Q(a)$ of the PIRM residuals $v(a)$ corresponding to (7) is given by:

$$v_Q(a) = P_Q(a) \underbrace{\left(P^\mu - S_Q(\omega, a) C^T C U^\mu\right)}_{=:\Phi_Q(\omega,a)}. \tag{13}$$

where $P_Q(a)$ is the projection to the orthogonal complement of

$$X_Q(\omega, a) := R(QS_\omega(a)Q^T\bar{C}^T) \underbrace{\approx}_{(11)} N(CQF_\omega(a)Q^T). \tag{14}$$

Under this assumption it follows that

$$v_Q(a^0) \approx 0 \tag{15}$$

because:

$$CU^\mu \approx C[QF_\omega(a^0)Q^T] \cdot \left(P^\mu\right) \tag{16}$$

$$CU^\mu \approx C[QF_\omega(a^0)Q^T] \cdot \left([QS_\omega(a^0)Q^T]C^T C U^\mu\right), \tag{17}$$

and thus

$$P^\mu - [QS_\omega(a^0)Q^T]C^T C U^\mu \in N(CQF_\omega(a)Q^T) \approx R(QS_\omega(a)Q^T\bar{C}^T) \tag{18}$$

$$\Rightarrow v(a^0) \approx 0 \tag{19}$$

The main advantage of $v_Q(a)$ in comparison to $v(a)$ is that the time consuming computation of $P(a)$ is substituted by the evaluation of $P_Q(a)$, which is much more efficient because of the smaller subsystem dimension $l \ll n$.

Since $v_Q(a^0)$ vanishes only approximately, $v_Q(a)$ is not well suited for the identification of the subsystem parameters corresponding to $Q$ if the couplings are more complex. But it is well suited for a local analysis of the system that takes only small deviation of the parameters from a healthy reference state (described by the start parameter $\mathbb{1}$) of the system into account. This is done in the next section by defining a damage indicator that is based only on the partial derivatives $\frac{\partial v_Q(a)}{\partial a_\nu}\Big|_{a=\mathbb{1}}, \nu = 1, \ldots, n_p$, of the subsystem adaptation of the PIRM residuals. This indicator will be illustrated by a realistic example considering real damage.

# 4 THE DAMAGE INDICATOR BASED ON PROJECTED SUBSYSTEM RESIDUALS

In contrast to parameter identification in damage detection the primary task is not the updating of the parameter components that have changed due to a time-variant behaviour of the structure, but to locate the damage that has caused this time-variance, i.e. to determine the damage related parameter components.

For this purpose an indicator-based analysis – as presented in the following – that may be applied online is more suitable than a time consuming identification procedure.

In the following $Q$ is a selection matrix for a given subsystem that is used for monitoring and damage detection. Since the partial derivatives

$$v_Q^{(\nu)}(a) := \frac{\partial v_Q(a)}{\partial a_\nu}\Big|_{a=\mathbb{1}}, \nu = 1, \ldots, n_p, \tag{20}$$

are very sensitive to structural modifications they are well-suited for this purpose and can be applied to this task by the following indicator definition:

$$\tau_\nu := \frac{\|v_Q^{(\nu)}(\mathbb{1})\|}{\|v_Q^{D(\nu)}(\mathbb{1})\|} \geq 0 \quad \text{for } \nu = 1, \ldots, n_p, \tag{21}$$

where $v_Q^D(a)$ are the projected subsystem residuals for the measurements $U_D^\mu$ of the possibly damaged structure but based on the same excitation $P^\mu$ as used for the undamaged case ($U^\mu$). The justification for $\tau_\nu$ being a damage indicator is as follows. In practice the enumerator of (21), $\|v_Q^{(\nu)}(\mathbb{1})\|$, which should theoretically be 0, is not equal to zero: due to measurement errors and imperfect parameter components of the start model $\mathbb{1}$, $\|v^{(\nu)}(\mathbb{1})\|$ is in general a real number greater than zero which reflects the last reference-state of the structure. This reference value for the healthy state is then compared via $\tau_\nu$ with the corresponding gradient norm $\|v_Q^{D(\nu)}(\mathbb{1})\|$ based upon the measurements $U_D^\mu$ that are taken from the (possibly) damaged structure and also contain similar measurement errors and imperfections than $U^\mu$. If no damage has occurred, $\tau_\nu$ will take a value near 1 since then we expect $\|v_Q^{(\nu)}(\mathbb{1})\| \approx \|v_Q^{D(\nu)}(\mathbb{1})\|$. The other case is $0 < \tau_\nu \ll 1$, i.e. $\|v_Q^{(\nu)}(\mathbb{1})\| \ll \|v_Q^{D(\nu)}(\mathbb{1})\|$, and hence the parameter component $\nu$ is indicating a damage associated to parameter $\nu$.

An application of this indicator is presented in the next section.

# 5 Application

## 5.1 Description of the structure and the experimental design

The presented method was applied to the damage diagnosis of the steel frame construction of the gantry robot. Figure 1 shows a photo of the robot used in the investigations. This robot performs transportation tasks within a manufacturing centre which consists of two lathes and two storage magazines. The equipment that constitutes the manufacturing cell determines the size of the frame construction that is 6.00 m × 8.00 m × 2.94 m (3.36 m). The structure consists of steel beams with hollow rectangular cross-sections. Such a construction was subjected to impact excitation during the investigations. The dynamic test included two stages:

1. Impact test of the undamaged structure,
2. Impact test of the structure after the introduction of the damage.

The damage consisted in loosening bolts that connect the crosswise stiffening beam with the horizontal beam (see figure 2).

The location of the damage is also marked in figure 3 that presents the model and the location of the excitation force and accelerometers. Both tests were technically identical, which means that the same design of the experiment was used in both cases as well as the same parameters were used during the acquisition and processing of the signals. The excitation was located at the column which is marked by an arrow in figure 3. The excitation force was produced by a impulse force hammer type. During the experimental investigations 4 tri-axial piezoelectric accelerometers type were used. These 4 sensors were moved after taking the measurements to the new positions as to obtain the measurements in all the 98 experimental nodal points as shown in figure 3. Each measurement included 10 averages for a better accuracy of the calculated frequency domain characteristics that is auto-power

Figure 1: The structure under investigation: A gantry robot

spectrums, coherence functions and frequency response functions (FRF). Uniform and exponential windows were applied to the force and acceleration signals respectively to improve signal to noise ratio. The sampling frequency was equal to 2048 Hz.

On the basis of the experiment 294 FRF (3x94) were obtained for both undamaged and damaged structure. These characteristics were directly used for the detection of the damage. for healthy and damaged structure are shown in the figure 4.

Since the acceleration signals were used for the calculation of FRF they were integrated in the frequency domain to produce the displacement type signal according to the equation:

$$H_D(j\omega) = \left(\frac{1}{j\omega}\right)^2 H_A(j\omega) \tag{22}$$

Such signal can be directly used for the determining the damage indicator. FRF calculated as the ratio of the displacement spectrum to the force spectrum can be treated as the response of the system to the unit force excitation. Thus, in consequences $U^{M_1}$ and $U^{M_2}$, the displacements corresponding to the healthy and damage structures respectively are replaced by the frequency response functions measured at healthy and damaged structure. The excitation force remains constant and is equal "1" for all frequency components considered during the computations of the damage indicator. The method requires also the construction of the model. The system matrices $M, B, K$ are used for the evaluation of the projected input residuals as defined in equation (13). The important issue is that the damage indicator defined in (21) does not require the construction of the model which describes the mass-damping-spring properties of the damaged structure but only the model which corresponds to the undamaged object.

The finite element model of the considered frame construction was built in such a manner to allow further changes focused on model updating. The model was constructed by means of the finite element method. The FE model of the structure was produced using the structural dynamics toolbox (SDT) of Matlab. The model consists of quad4, tria3 elements and one

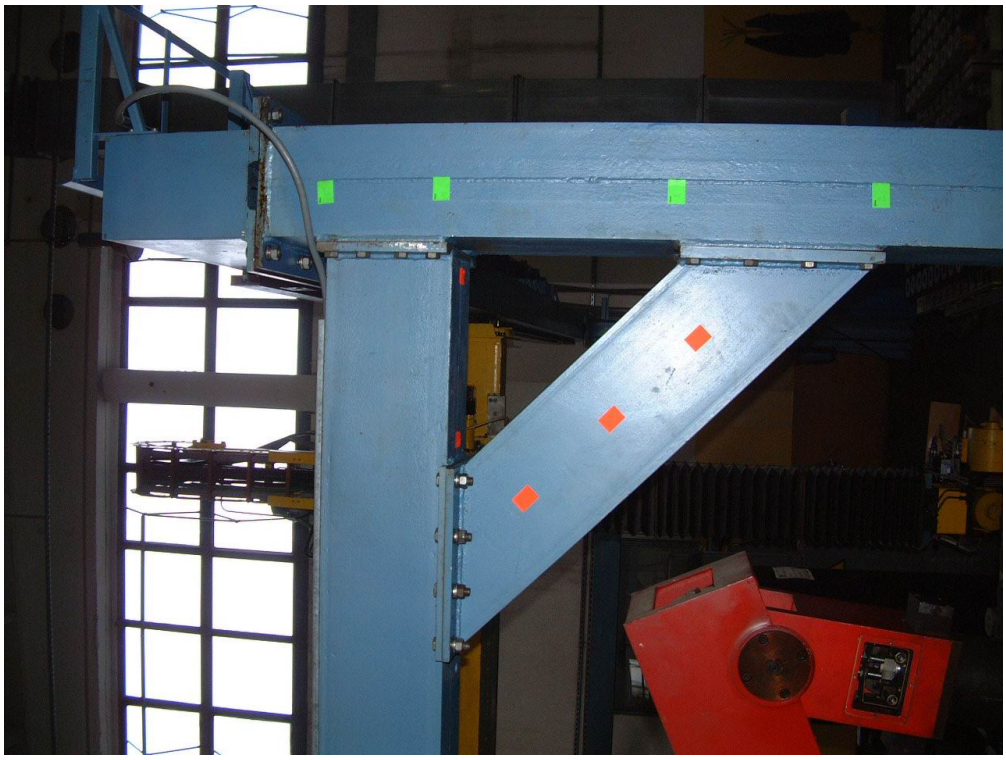

Figure 2: Location of damage, i.e. loosend bolts that connect the crosswise stiffening beam with the horizontal beam

lumped mass for the modelling of the robot's gripper.
The material properties of every element, except contact elements, in the initial model were:

**young modulus:** $2.1 \times 10^5$ Mpa,

**density:** 7800 kg/$m^3$.

The thicknesses of the finite elements of the particular constructional parts of the structure are as follows:

**long beams and vertical columns.** 0.01 m,

**short beams:** 0.005 m,

**crosswise beams:** 0.004 m.

A lumped mass of 400 kg was added to simulate the influence of the gripper on the object dynamics.
The dimensions were assumed on the basis of the technical documentation of the robot and direct measusrements. The contact joints between the constructional elements and also between the vertical columns and the ground were used as updating parameters. The contact joints were modelled as thin layers with significantly lower Young modulus and density than steel. Thus, thickness, Young modulus and density of the contact joints were used to tune the model to the results of the experimental investigations, i.e to obtain the used start model parameter $\mathbb{1}$ describing the healthy state of the system. Remember that $\mathbb{1}$ is necessary to evaluate the damage indicator $\tau_\nu$ as defined in eq. (21). The FE model was updated to obtain a good correlation with the modes that were well excited during the experimental investigations of the healthy structure.

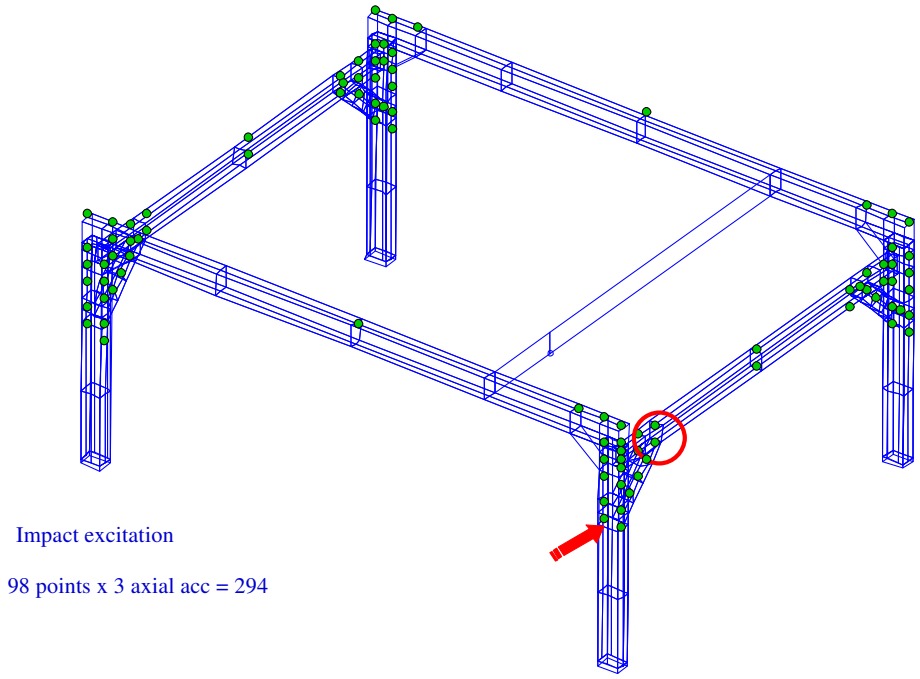


Figure 3: Location of the damage and the measuring and excitation points

They were selected on the basis of the SUM characteristic which is shown in figure 4. The set of the considered eigenfrequencies includes the following natural frequencies: 18 Hz, 44 Hz, 78 Hz, 88 Hz, 129 Hz.

The final step concerning model preparation is its division into geometrically defined regions. The structure is divided into subsystems for which damage indicator values are calculated. For our application the subdivision consists in the construction of a separate subsystem for each of the $n_p$ parameter components as shown in figure 5. The subsystems matrices that satisfy the equation (1) where also created. While dividing into subsystems one has to take into account the location of the sensors during experimental tests since each region must include at least one measured FRF. Having this in mind the investigated frame construction was divided into 16 regions as shown in figure 5. The stiffness and inertia matrices were built for all of the subregions. The dynamic stiffness matrix (see eq. (3)) is then expressed as a linear function of the dimensionless parameter that are assumed to be equal 1 for the model describing the healthy state of the structure ($\mathbb{1}$).

## 5.2 Results

The results of the experimental measurements and the subdivided model of the healthy structure is used for the calculation of the introduced damage indicator. The computation included 5 scenarios that included different frequency components for the calculation of the damage indicator. In general the selection of the frequency components was based on the observed significant differences between SUM functions (figure 4) calculated for the healthy and the damaged state of the structures.

In the first scenario the damage indicator was calculated at the single frequency 78 Hz. The results are shown in the figure 6. The lowest value of the indicator was obtained for the region number 3 that correspond to the location of the loosened bolts. The second lowest

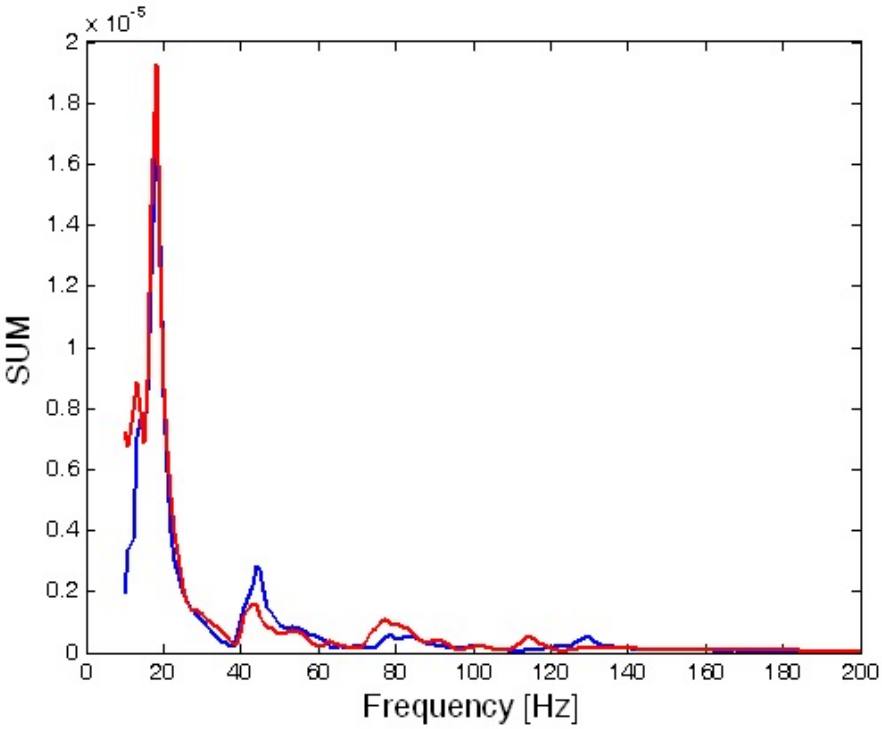


Figure 4: Sample frequency characteristics (red line=damaged state, blue line=healty state) obtained taking the sum of the characteristic of all nodes (y-axis).

value of the indicator is for the region number 1 which includes also the crosswise stiffening beam. The behaviour of this element was influenced at most by the introduced damage.

The second scenario was enhanced by the additional consideration of the frequency 114 Hz (fig. 7). The results are very similar to those obtained during first approach. The consideration of the frequency bands $75 \ldots 78, 113, 114, 115$ Hz also produces comparable values in scenario 3 (see figure 8). The fourth scenario considers frequencies 44, 78 and 114 Hz and thus is qualitatively different in comparison to the previous ones since the SUM function of the damaged structure (red line in figure 4) exhibits smaller values at 44 Hz than the healthy structure; and this is in contrast to the frequencies 78 and 114 Hz where the healthy structure exhibits smaller values. Again, the obtained results as shown in figure 9 are indicating the location of the damage in subsystem 3.

The fifth scenario included all significant frequency components of the measured FRFs, that are 18 Hz, 44 Hz, 78 Hz, 114 Hz and 119 Hz. Once again the values of the damage indicator located correctly the fault of the system within the region number 3 (see figure 10).

# 6 CONCLUSIONS

The paper is about model based parameter identification and damage localization of elastomechanical systems using input and output measurements in the frequency domain.

An adaptation of the Projective Input Residual Method (PIRM,[3]) to subsystem damage identification is presented. For this purpose the PIRM residuals were adapted with respect to a given subsystem to be analysed. Based on the gradients of these projected subsystem residuals a damage indicator was introduced which is sensitive to parameter changes and structural damages in a given subsystem. Since the computations are done w.r.t. the smaller dimension of a subsystem this indicator shows a computational performance gain compared

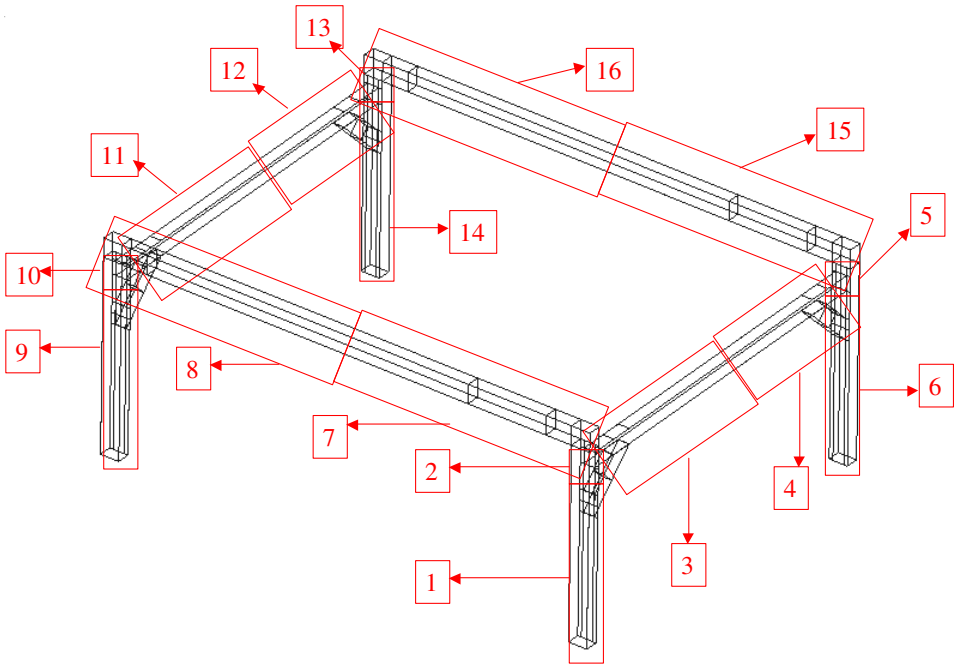


Figure 5: Subdivision of the model into regions/subsystems

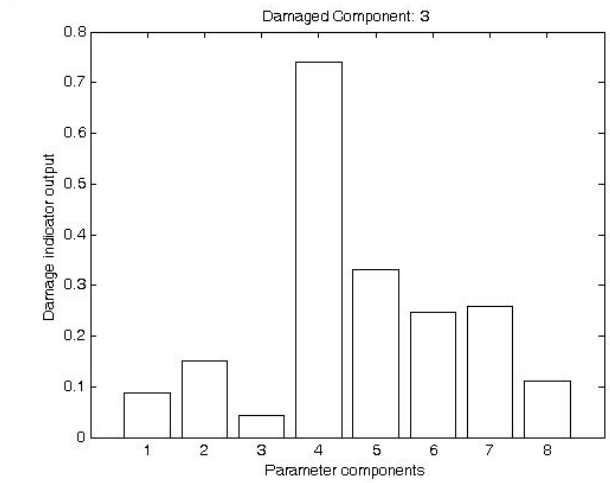


Figure 6: Results of scenario 1: x-axis = parameter components, y-axis = indicator values

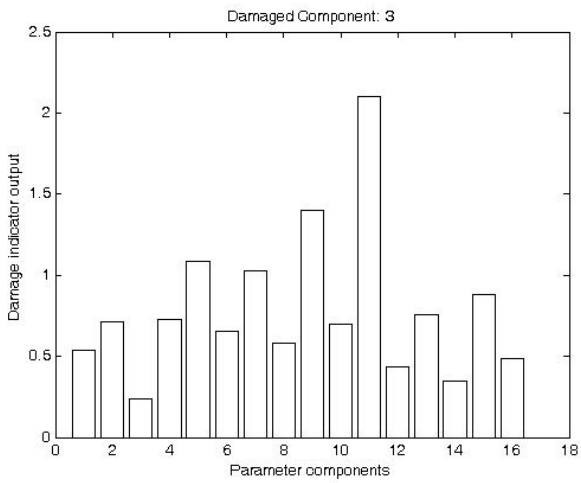


Figure 7: Results of scenario 2: x-axis = parameter components, y-axis = indicator values

to the non-subsystem approach. This gain in efficiency makes the indicator applicable in online monitoring and online damage diagnosis where continous and fast data processing is required.

The presented application of the indicator to a gantry robot could illustrate the ability of the indicator to indicate and locate real damage of a complex structure.

Since in civil engineering applications the system input is often unknown further investigations will focus on the output-only case since the generalization of the presented methods to this case will broaden the application spectrum of the method.

**Keywords**: System identification, damage location, incomplete measurements, projection

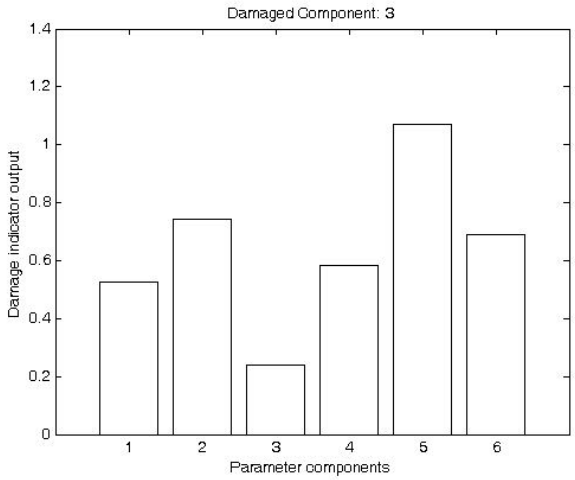


Figure 8: Results of scenario 3: x-axis = parameter components, y-axis = indicator values

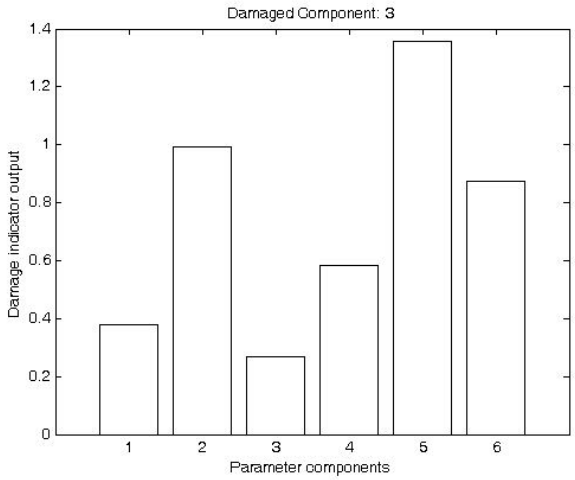


Figure 9: Results of scenario 4: x-axis = parameter components, y-axis = indicator values

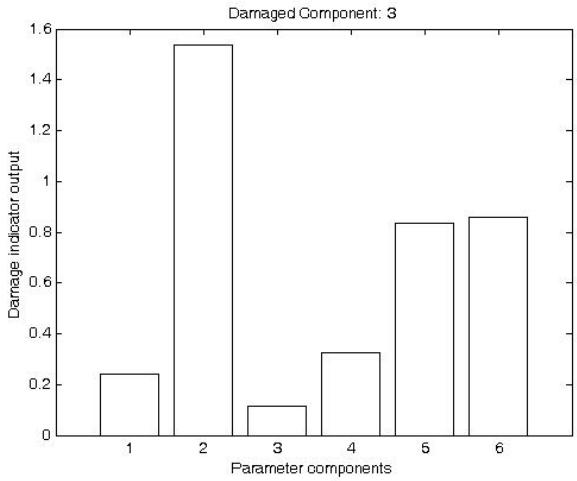


Figure 10: Results of scenario 5: x-axis = parameter components, y-axis = indicator values

methods, damage indicator, non-linear parameter estimation.

# References

[1] M. Oeljeklaus. The Linear Output Residual Method with Computationally Adaptive Excitation in the Frequency Domain – I. Theory. *Mechanical Systems and Signal Processing*, 11(5):725–741, 1997.

[2] M. Oeljeklaus. The Linear Output Residual Method with Computationally Adaptive Excitation in the Frequency Domain – II. Application. *Mechanical Systems and Signal Processing*, 12(2):243–258, 1998.

[3] M. Oeljeklaus. Projection Methods within Model Updating. In M. I. Friswell, J.E. Mottershead, and A.W. Lees, editors, *Identification in Engineering Systems*, pages 325–335. University of Wales, Swansea, 1999.

[4] H.G. Natke. Updating computational models in the frequency domain based on measured data: a survey. *Probabilistic Engineering Mechanics*, 3(1):28–35, 1988.

[5] H.G. Natke. *Einführung in Theorie und Praxis der Zeitreihen- und Modalanalyse.* Vieweg, Braunschweig, Wiesbaden, 1992.

[6] N. Cottin, H.-P. Felgenhauer, and H.G. Natke. On the Parameter Identification of Elastomechanical Systems Using Input and Output Residuals. *Ingenieur-Archiv*, **54**, 378-387, 1984.

[7] H.G. Natke and C. Cempel. *Model-Aided Diagnosis of Mechanical Systems, Fundamentals, Detection, Localization, Assessment.* Springer Verlag, 1997.

[8] M. Oeljeklaus and B. Povalka. A Projection Based Damage Indicator Working with Incomplete Measurements. In J.H. Zhang and X.N. Zhang, editors, *Proceedings of International Conference on Advanced Problems in Vibration Theory and Applications*, pages 249–256. Science Press, Beijing, China, 2000.

[9] M. Oeljeklaus and H.G. Natke. The Use of Projected Input Residuals in Damage Identification. In *Proceedings of the 3rd International Workshop on Structural Health Monitoring, Stanford CA, USA, 12.9.-14.9.2001.* Stanford University, CA 94305, USA, 2001.

[10] J. Dieudonné. *Grundzüge der modernen Analysis.* Vieweg und Sohn, Braunschweig, 1970.

[11] Rudolf Zurmühl. *Matrizen und ihre Anwendungen I.* Springer Verlag, Berlin, 6. edition, 1992. Springer-Lehr-Buch.